Performance Evaluation in a Radar System

Ahmed Alsheikhy, Muhannad Almutiry

Northern Border University, College of Engineering, Electrical Engineering Department, Arar, Saudi Arabia

Summary
In surveillance fields, radar is considered essential element or component. It is being rapidly used in remote sensing of large areas with capabilities of low vulnerability to electronic countermeasures. Tomographic process in radar systems can be defined as a process of 3D reconstruction in a measurement domain using several static distributions for a transmitter and a receiver. Using radar tomographic process suffers from strong sidelobes in the measurement domain by interfering with the echoes from weak scatters. Therefore, system's ability and performance to detect a certain target feature decrease. To detect and extract weak target features from radar tomographic imagery, a new method was developed. This paper presents a performance evaluation method using a framework to estimate an average response time through extracting the weak target features from radar tomographic imagery scheme. The framework can determine the bottlenecks of using the new method to increase the image quality in radar tomographic process. Numerical evaluation of the developed approach is included to prove its effectiveness.

Key words:
Hierarchical Performance Model (HPM), Response time evaluation, Scatters sidelobes, Radar tomography, Framework, Inverse problem, Radio frequency.

1. Introduction

Modern radar systems are used to detect, search and locate different objects. Radar systems use radiation to track or detect non particulate radiation objects [1,2,3]. Radars can be also used for surveillance purposes, speed estimation, identifying explosive devices [1] and tracking several objects. Radar systems can be deployed in several remote sensing applications [2,3,4]. Obtained images from radars is considered as Radio Frequency (RF) tomography [4]. Using multistatic radar imaging methods in numerous distributions of transmitters and receivers is the common feature being deployed and employed [4,5]. Multistatic radar imaging methods provide helpful information about the shape and edges of a target being monitored [4]. In radar tracking process, the imaging process uses electromagnetic radiation models to predict target echoes and even distance if necessary.
Radar tomography scheme is deployed in several applications such as Ground-Penetrating Radar "GPR", Inverse Synthetic Aperture Radar "ISAR" and building penetration [4,5]. Tomographic process suffers from masking weak scatters by near strong scatters. Numerous techniques were developed to enhance the image quality with help from strong scatterer echoes [4,5,6]. A CLEAN algorithm is the most common method being used to suppress the dominant scatterer. The CLEAN algorithm is developed based on estimating the point spread function using either radiation pattern or image response of the dominant scatterer to remove it from received wave [4]. Removing the dominant scatterer points decreases the Sidelobe effect in the radar images [4,5,6,7]. In radar tomographic environments, a set of distributed transmitters uses known waves to radiate an area of interest [5,6,7]. Using known waves invading upon targets produces several levels of scattering fields which are related to the shape of the targets linearly.
M. Almutiry et al in [4] developed a method based on a unique electromagnetic model to extract weak target features from radar tomographic images. The developed scheme improves the image quality by suppressing the weak scatterers. More information about the developed approach in [4] is presented in section 3. Many positions of targets can be viewed using radar tomography due to the spatial distribution of transmitters and receivers [4,5]. The method in [4] is represented as a 3D contrast function which has a value bigger than zero between the target and the surrounding free space. Born approximation is also used iteratively to suppress weak scatterers one at a time in order to remove the effect of multiple dominant scatters since the developed model is still linear.
Our contribution in this paper is done by using mathematical equations model, included in the framework shown in fig. 1, to estimate the average response time for the developed algorithm in [4]. The response time is defined as a time interval between receiving the input until the appearance of the output.
Performance evaluation, such as response time, at an early stage is considered very crucial to avoid unexpected results in the final implementation of a system under investigation. The framework used, to evaluate the average response time for developed scheme in [4], as illustrated in fig. 1 is composed of 3 components which are a functional modeling approach, which is represented by a Hierarchical Generic Finite State Machine "HGFSM", a Markovian Model and an analytical approach which is represented by HPM. The output from the framework can be seen as the objective function(s). More information about the framework is found in [15,16]. The framework is also used to spot any bottleneck in the system. These bottlenecks cause delay in the response time. This helps designers to improve the

Manuscript received November 5, 2018
Manuscript revised November 20, 2018

system performance. In this paper, system performance refers to the response time. Estimated average response time is compared with the average actual one within this paper to show the difference between them and to illustrate the validation of the framework being used. The difference between the average actual and the predicted response time lays within ± 9% which is considered acceptable rate.

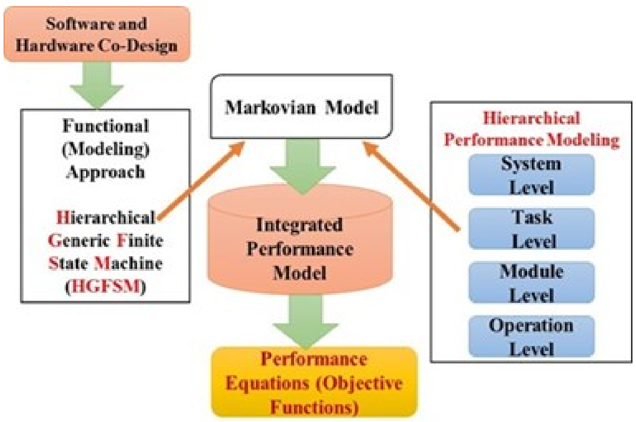

Fig. 1 Developed framework

In the reminder of this paper, we present related work on performance evaluation and estimation of radar systems in Section 2. Section 3 provides a detailed discussion of the developed approach in [4] and the framework to estimate the average response time. Section 4 includes numerical evaluations of the developed method in [4] and the bottlenecks location(s) found by the framework. Conclusion and future work are in section 5.

2. Related Work

Radar systems use several scientific subjects such as estimation, tracking/detection and electromagnetic waves to manage different resources available in the system under consideration [4]. Several performance analysis estimations for radar systems have been performed and conducted to study how they react under severe circumstances.

Y. Li et al in [3] conducted performance evaluation of target detection in vehicle-born radar in blackout condition. Near-Space Vehicle-Born Radar "NSVBR" is considered a new installation method of radar systems [3]. Investigation on the effect of blackout on electromagnetic waves is performed first. Then, three performance indexes on the detection capability and two indexes on the robustness are conducted. These performance evaluations focused on providing more information on the detailed of the detection process. The authors claimed that the proposed method was very helpful for designers of radar systems and even users. NSVBR is more suitable in complicated scenarios as proven in the literature [3]. Performance evaluation indexes scheme performed can be seen the probability prediction evaluation of detection process. Statistical methodologies are also used in the developed scheme, two important parameters were neglected. Radar transmitted power plays a significant role in affecting the strength of the signal being transmitted to the radar receiver. The authors proposed a novel metric evaluation, using the ration of the probability of the detection process to the product of the transmitted power with the target's RCS, which was used to refer to the normalization procedure of the probability operation. RCS refers to the Radar Cross-Section. All previous three parameters were combined to form one index used to characterize the performance in several technical specialties. Interested readers are referred to [3] for more information. Three scenarios were conducted using the proposed method to evaluate the probability indexes of the detection procedures, however, the performance evaluation within this paper estimates the average response time needed to produce the output based on different levels of abstraction.

A. K. Shrivas and A. Mudakiar conducted a performance evaluation of radar systems in [8]. They described the analysis of Signal-to-Noise Ration "SNR" versus the various detection processes for several values of RCS for different modes of recent measuring systems. In addition, they measured the accuracy of their analysis based on an interest of a client and a provider. They claimed that their evaluating was mathematically rigorous, precise and efficient as desired and needed. First, a target's vary parameter "R" is computed by measuring a time delay, a time that a pulse takes to travel in the two means path between the radio detection and ranging of the target, to compare it later with the SNR values obtained. Matlab platform was used to develop a simulation in order to conduct a comparison between the radar vary equation "R" with the SNR values for several selection of parameters such as RCS and the peak transmitted power. Furthermore, the simulation helped the author to discuss the effect of the radar vary equation "R" on the low pulse repetition frequency and high pulse repetition frequency. Several mathematical equations were used during the evaluation process; however, the authors did not mention the effect of different levels of abstraction on their analysis. The framework used within this paper evaluates the average response time based on 4 levels of abstraction as shown in fig. 1, right hand side.

In [9], a series of defined tests were conducted to provide a detailed analysis of a radar system at distinct levels. Three levels were included. In fact, it was only one main level, then it was divided into two more sublevels for deep details. The top level, the main level, was used to assess the quality of information "data" being gathered by the radar sensors by measuring the overall performance of the sensor against the performance parameter reference values within a specific standard such as EUROCONTROL. The second level provides depth evaluation of the technical performance of the individual components of the sensors such as Antenna, Extractor and Receiver. The last level, which is the bottom one, is used to generate a specialized series of defined tests in order to optimize the radar system. More information about the conducted tests with their requirements can be found in [9]. The framework used herein this paper uses four levels of abstraction to capture all required information needed to evaluate the system performance. Most of the performance evaluation conducted earlier focused only on the system level and neglected the effeteness of other levels such as task level, module level and operation level as illustrated in fig. 1.

L. K. Cunha et al in [10] performed an early performance evaluation of the Dual-polarization radar for rainfall estimation in two distinct cities in the USA using two overlapping radars. The two cities were Kansas City, Missouri and Topeka, Kansas. The study areas were located in different distances from the two radars. The authors concluded that the improvement in the rainfall estimation achieved by polarization radar were not consistent for all events or even radars. During the evaluation procedures, two rainfall fields were developed which were SPR and DPR over an approximately area of 3600 km2. SPR refers to Single-Polarization S-band Radars whereas DPR stands for Dual-Polarization S-band Radars. The main objective for the proposed evaluation in [10] was to assess the improvement obtained by DPRs in order to explore the potential of applying the available dataset on Urban Hydrology areas when ground data is not existed. Initially, the rainfall estimation is performed without removing the systematic biases relative to rain gauges which requires long dataset. Then, Normalized Bias “NB”, Standard Error “SE” and Pearson Correlation coefficient “CORR” parameters are determined. The CORR parameter gives a hint of a degree of linear association between the radar and gauge readings. March, May and September 2012 storm events were exhibited and used in the evaluation procedures. More information about the evaluation can be found in [10]. In this paper, Matlab platform is used to compute the average actual response time and average predicted one after performing several experiments and measurements.

In [11], C. Du performed performance evaluation and waveform design for Multiple-Input Multiple-Output “MIMO” radars since they have been receiving increasing attention in recent years. First, a model for finite scatterers was developed based on which a target detection performance of a MIMO radar with arbitrary array-target is analyzed. Then a hybrid bistatic radar is introduced which combines MIMO radar configuration with the phased-array to speed up the process of a coherent gain and a spatial diversity gain simultaneously. Lastly, two new phase radar methods, which involve signal retransmission, is developed to estimate a desired performance metric. The performance metric referred to the detection performance as other studies conducted in the literature. A system model to improve the performance of detection process was developed based on the independent finite number of small scatterers by exploiting spatial diversity. The developed model works on deriving the theoretical probability of detection for the system under consideration according to the arbitrary array-target configurations. Monte Carlo Simulation technique was used to validate the developed model which helped in predicting the detection performance. The framework within this paper estimates the average response time as the desired performance metric since determining the time needed to produce the output is more crucial in several applications such as tracking or detection.

S. Zeng in [12] performed performance evaluation of automotive radar systems using carrier-phase differential GPS. The performance evaluation in [12] refers to a centimeter-level ground-truth system by creating objective test procedures for the radars. A developed effective scheme to handle signal attenuation or blockage was used to achieve the performance evaluation based on GPS relative positioning. Two vehicles were used and considered in the developed ground-truth system, two mount GPS receivers were put on the roof of each vehicle. Several radars were mounted behind the front and back bumpers in a host vehicle with 30 meters as maximum sensing range. The developed scheme was working as an independent measurement system. The performance evaluation in [12] requires different hardware tools and which is very costly in terms of time needed to install, set up and perform the experiments and also the fund needed to prepare all required hardware. However, the framework herein this paper saves time and financial fund since only knowledge in mathematical with a pencil and paper are required and needed.

3. The Developed Framework

Geometric diversity of tomographic radars increases the information obtained from a measurement domain due to the spatial distribution of transmitters and receivers [4,5,6,7]. For the developed algorithm in [4], a target may be surrounded by multiple dipole transmitters (N) and multiple dipole receivers (M) to image the target. A transmitter n is located at rrn and associated with a polarization âtm, the same thing applies on a receiver m as depicted in fig. 2 for single pair.

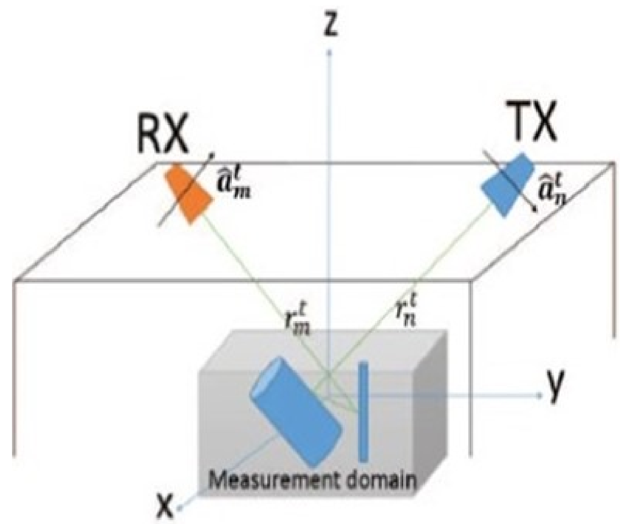

Fig. 2[4] 3D model of the tracked target of interest

According to fig. 2, the transmitter radiates a waveform while the remaining transmitters are in inactive mode. The receivers gather echoes from the target, a position of each receiver is known based on a determined fraction of the wavelength. Noise and even clutter are removed from the collected data in order to store it. A simple forward and inverse model for the tomographic radar was developed for the time-harmonic electric field. Fourier transformation and a stretch processing method were used to come up with the developed forward scheme. The scattered field Es(rtn,rrm) for any transmitter n and any receiver m using the Born approximation approach within the measurement domain which is assumed to be a free space medium is computed as follows:

$$Es(rtn,rrm) = k02\iiint[\hat{a}tm*\breve{G}(rrm,\acute{r})] * [\breve{G}(\acute{r},rrn)*\hat{a}tn]^{t}Ţ(\acute{r})d\,\acute{r} \quad (1)$$

In eq. (1), k0 is the wavenumber, Ţ(ŕ) represents an unknown contrast function with ŕ represents a position vector while Ğ(rrm,ŕ) refers to the Green's function. The Born approximation as stated in [4] is linearly related to the contrast function which can be represented as a matrix multiplication which is used to develop the forward model scheme. The unknown contrast function is computed using an operator L which is always ill-conditioned as mentioned in [4]. The operator L is determined by applying the Algebraic Reconstruction Technique "ART", more information about ART is found in [4]. The eigenvector u and eigenvalues γ are easily determined after applying ART method such that

$$D = \gamma u \quad (2)$$

where D is the cell's vector representation. The eigenvectors and eigenvalues are used to estimate the polarization and magnitude needed for the dominant scatterers. Three eigenvalues exist in each cell, the estimated values of the polarization and magnitude are contained in the largest eigenvalue γ. A flowchart in fig. 3 from [4] illustrates the forward approach used to extract weak target features from radar tomographic imagery.

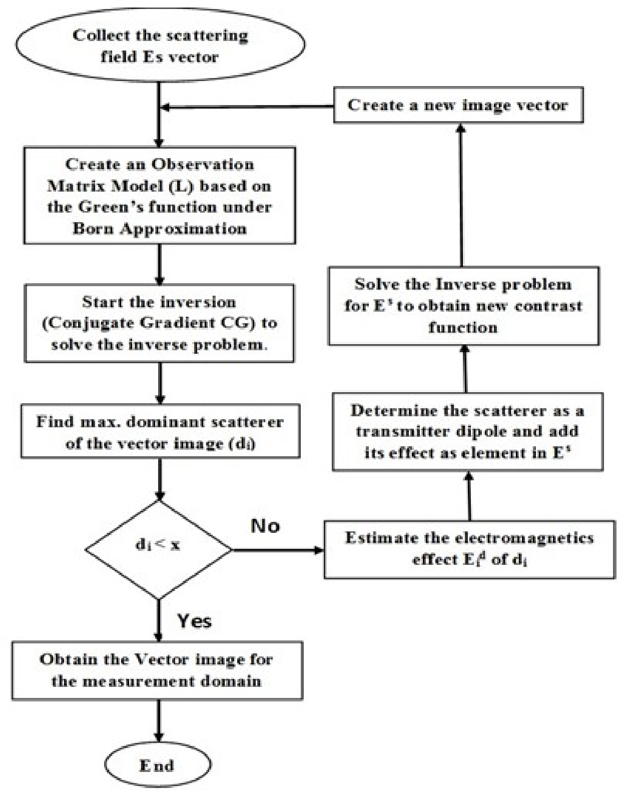

Fig. 3 The flowchart for the developed scheme in [4]

In fig. 3, x denotes the threshold value. The maximum eigenvalue that is larger than a determined threshold helps locating the dominant scatterer in the reconstruction array. The scatterer estimated and located is modeled later as dipole which is treated as an extra transmitter. The interested readers are referred to [4] for more information about the developed algorithm. The forward technique developed in [4] generates a series of reconstruction images, each reconstruction component shows clearer picture of the weaker scatterers. All generated reconstruction images are combined into a single image which illustrates both scatterers, the strong and the weak.

The Developed Framework

The framework as depicted in fig. 1 is composed of three components which are the HGFSM, Markovian Model and HPM as stated earlier. In fig. 1, the HGFSM is in the left-hand side, the Markovian model is in the top middle and the HPM is in the right-hand side. The developed HGFSM consists of three levels, also known as layers, with a total number of states equal to 16 states. These are used to capture all required information in order to ease and smooth the analytical analysis. Fig. 4 illustrates a general overview of the HGFSM.

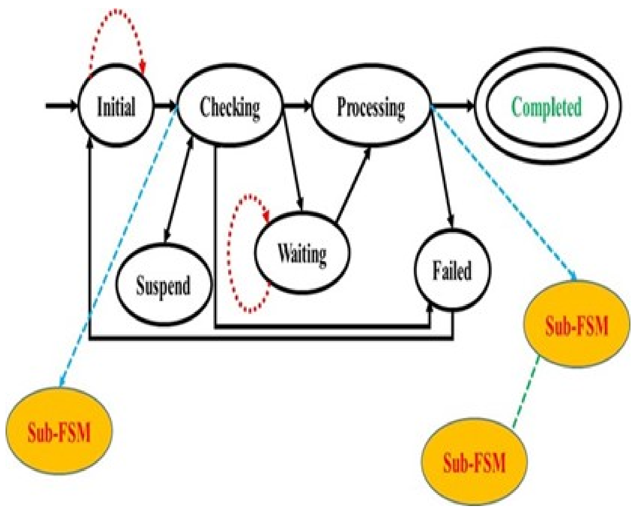

Fig. 4 General overview of the HGFSM

Self-loop in the Initial state indicates that there is a malfunction, hence, the radar is unable to process its input while the self-loop in the Waiting state implies that a task waits its turn to be gained and processed by a Processing Unit "P.U.". Each sub-FSM is composed of three different states, so there are 7 states in the Super "higher" level of the framework and 9 sub-states in the lower level to the form the hierarchy model. Note that the Suspend state can be included also in the Checking state if needed. The interested readers are referred to [15,16] for more information about the developed framework and operations take place in each state. The HGFSM is then converted into the Markovian model which is later used to integrate with the HPM to perform the required analytical analysis to estimate the average response time. Fig. 5 demonstrates the hierarchy model of the HGFSM. Super FSM in fig. 5 refers to the GFSM illustrated in fig. 4. Each subscript represents the index for every sub-FSM, however, they are totally internally different.

Performance modeling evaluation is considered to be the abstraction of the functional and performance characteristics of a system which are combined to determine if it meets performance requirements based on a user demands and system architectures [15,16,18,19]. The Hierarchical Performance Model (HPM) is illustrated in fig. 6 from [15].

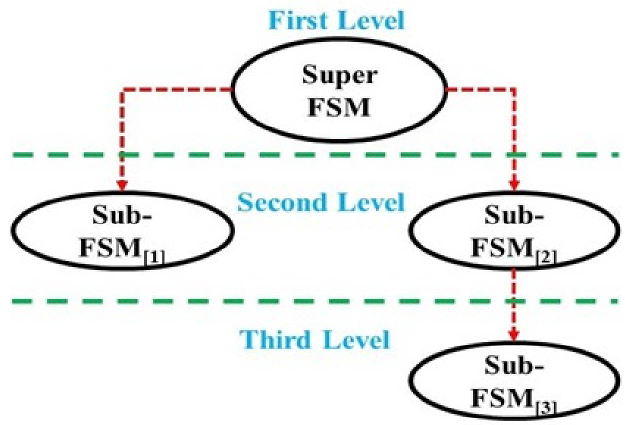

Fig. 5 Hierarchy model of the HGFSM

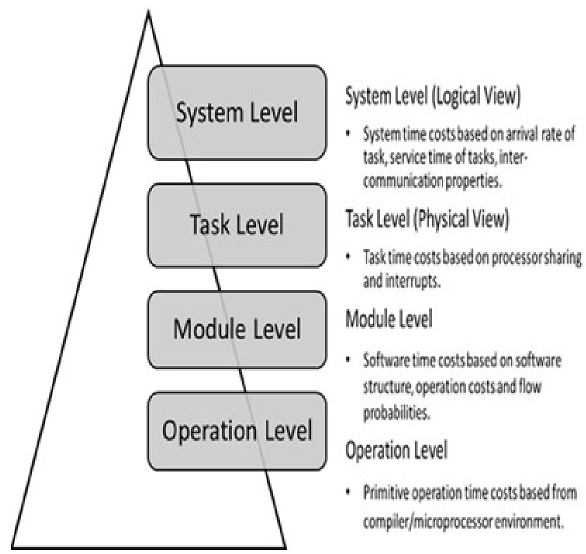

Fig. 6 The hierarchical performance model layers "levels"

More information can be found in [15,16,18,19] for HPM. Each level represents a different abstraction layer which is used to propagate the required information from the bottom layer to the higher layer in order to derive the objective function(s). several factors exist in each layer which influence the derived equation to obtain the average performance metric which is determined in this paper as the response time. Inside the framework, different conditions or circumstances are performed to determine where a task must be forwarded. The objective functions are derived from the CFG which is not shown due to the space limitation. The performance equation "objective function" for the framework is as follows:

PE

= (1*Cinitial)+((1+e4)*(Ccheck+Ctest))+((e11+1)*Cdecision)+((e8 + e9)*(Cwait + Ctest))+(e11 + 1)*(Cexe + Ctest) (3)

In eq. (3), PE refers to the Performance Evaluation which represents the estimated response time value [15,16,18,19]. In addition, each parameter in eq. (3) is associated with its flow variable which is denoted by a variable "e". Every flow variable determines a value of moving through a path from a start node to an end node in the CFG [15,16]. Furthermore, it takes a value between {0,1, …., ∞}, also it mainly depends on a type of distribution being used and implemented [15,16,18,19]. The flows also represent the data dependent aspects of the computation time [15]. All flows "e" are discrete random variables and are modeled using probability distribution and statistics methods [15,16,18,19]. The most known probability distribution being used are summarized as follows:

- Bernoulli distribution.
- Binomial distribution.
- Geometric distribution.
- Modified Geometric distribution.
- Poisson distribution.

Each distribution is associated with a unique formula to determine the probability "P" value, In this research, equally likely event is assumed which implies that p = q = 0.5 so p + q = 1. Given the probability distribution type of e, several characteristics such as **Expected value** *E(e)*, **second moment** *E(e2)*, **Variance** *Var(e)* and the **coefficient of variation** C^2 are easily obtained [15,16].
To derive performance equations, also known as the objective functions, a software structure is used which determines the order of operations execution [15,16]. The software structure is seen as a **C**omputational **S**tructure **M**ethod "**CSM**", which consists of a **D**ata **F**low **G**raph "**DFG**" and a **C**ontrol **F**low **G**raph "**CFG**". The DFG for the framework is a regular flow chart as depicted in a figure which is omitted due to space limitation.
To be able to determine the estimated value for each state, all operations happen there must be known and can be obtained from designers. For developed algorithm in [4], a mapping scheme between the framework and the approach in [4] is proposed as follows:
In the Initial state: the algorithm starts by forming a radio frequency image when inverting a linear operator "*L*" using the Born approximation technique [4]. The resultant matrix is the eigenvalue one for the scatterers magnetic field for each cell. All radar systems are assumed to be in normal mode which implies that the systems run perfectly, hence there is no malfunction. Thus, the cost "C", associated with the self-loop, is ***zero***, only one operation happens there.
In the Checking state: the developed method in [4] finds the maximum dominant factor scatterer of the image vector in the reconstruction array which is treated later as a dipole. Then a threshold value is compared with the maximum scatterer factor to locate the dominant one in the reconstruction array using the eigenvalues. The corresponding resultant matrix is represented as a polarization matrix.
In the Waiting state: since the tomographic radar is considered as a real-time system since the waiting time must be very small which can be neglected, hence, the waiting time value is assumed to be "zero". Thus $C_{Waiting} = 0$.
In the Processing state: The rest of the developed approach in [4], also known as the forward method, as illustrated in fig. 3 takes place in the processing state. The algorithm stops when there is no value bigger than the predefined threshold, the output matrix contains both the strong scatterers and the weak ones. Fig. 7 illustrates the mapping scheme between the forward model in [4] and the framework used herein to estimate the average response time. Mathematically,

$$C_{Initial} = C_{contrast\ function\ energy} = C_{forming\ radio\ frequency\ image\ vector} \quad (4)$$

$$C_{Checking} = C_{applying\ MRL\ method\ to\ iteratively\ compute\ the\ contrast\ function\ energy} + C_{compare\ with\ the\ predefined\ threshold} \quad (5)$$

$$C_{waiting} = 0 \quad (6)$$

$$C_{processing} = C_{determining\ Gaussian\ distribution\ of\ target\ absent} + C_{statistical\text{-}analysis\ for\ each\ pixel} + C_{suppress\ and\ exploit\ the\ sidelobe} + C_{Gaussian\ noise\text{-}distribution} \quad (7)$$

C_{test}: can be determined using "if statement" to decide which a branch should be taken, either true or false. Previous equations from (4) to (7) are substituted into eq. (3) to estimate the PE value.
To determine the value for all flows "e" in eq. (3), equally likely assumption is considered so in "if statement", either the true branch or false branch has a chance of 50% to be taken. All previous equations from (3) to (7) determine the ***Expected Service Time values "E[s]"*** which is used later in a Node View in the system level. Interested readers are referred to [19] for more information about the details of the Node View.
Finding Number of Visits "***V***" in each state is considered as the next step. ***V*** is computed as follows:

$$[V] = (I-P)^{-1} \quad (8)$$

Where [V] is a matrix whose elements indicate number of visits to each state; the number of its entries is equal to the number of states exist in the framework. I is the identity matrix and P is the matrix of transition probabilities between all states. So the **A**verage **P**erformance **E**valuation "**APE**" is computed as:

$$APE = \sum (Vi * Ci) \quad (9)$$

i = 1, …….. ,6 which is number of states in the system which is represented herein as a modified framework; Ci indicates the value of cost associated with each state. In the modified framework, the Suspend state is included in the checking state, more information about it is found in [15,16]. Matlab is also used to determine the Number of Visits "V" in each state. Fig. 7 demonstrates the mapping "bridging" between the developed framework and the scheme mentioned and used in [4].

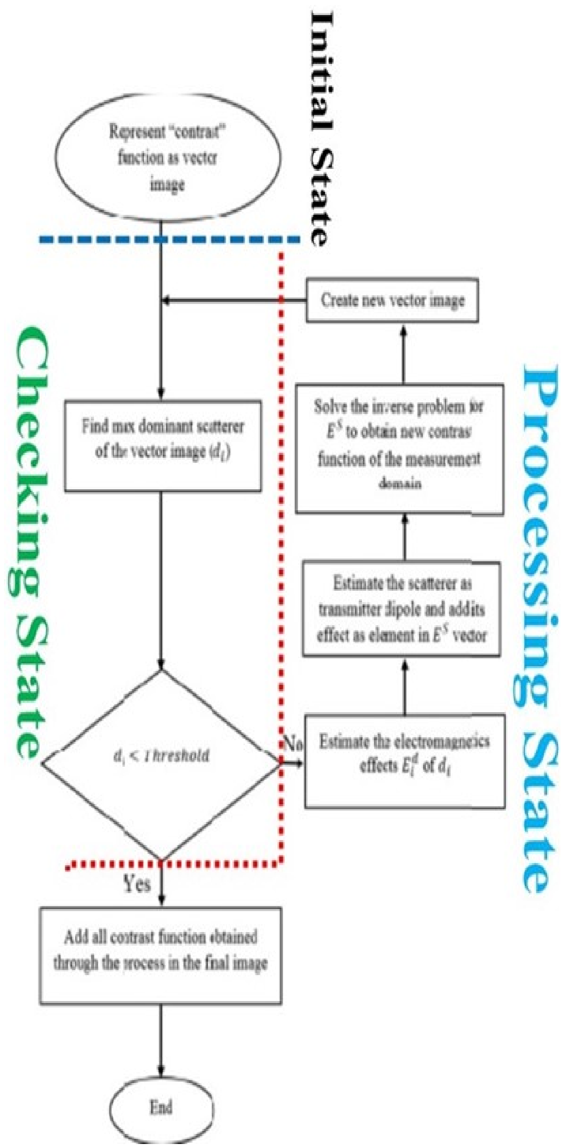

Fig. 7 Mapping approach between the framework and the forward model

4. Numerical Simulation Evaluations

Three different scenarios were performed to obtain the scatterer fields $\boldsymbol{E}^s$. We used a soft package named **FEKO** which was developed by Altair Engineering. It is used for electromagnetic field analysis of 3D. Reconstructing the contrast function of all three scenarios were performed using the radio frequency tomographic imaging principles. The preliminary results obtained by the simulation indicated that the developed algorithm in [4] was useful to reconstruct tomographic images in order to extract weak target features.

Experiment:

Two cylinders with different radius were considered in this experiment, the distant between two objects, the cylinders, was approximately 5cm along x-axis as depicted in fig. 9. One cylinder with radius = λ/4 placed in the center while the other cylinder had radius of λ/50, which is shown as a tiny object in fig. 8. The bigger cylinder was considered as the dominant scatterer which was incorporated into the forward model.

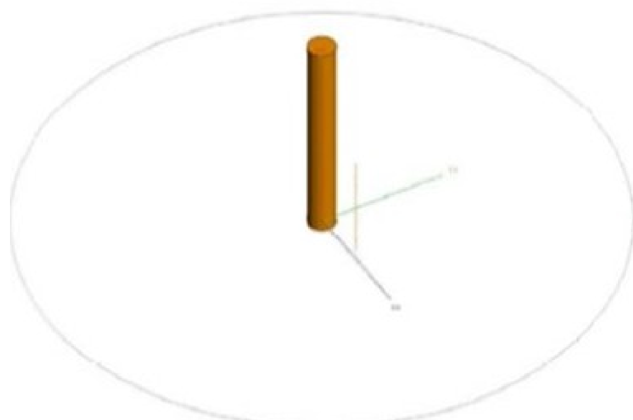

Fig. 8 Two objects placed in the measurement domain

The eigenvalues and eigenvector analysis were carried out to estimate the phase and magnitude of the dominant scatterer after locating its position as illustrated in fig. 9.

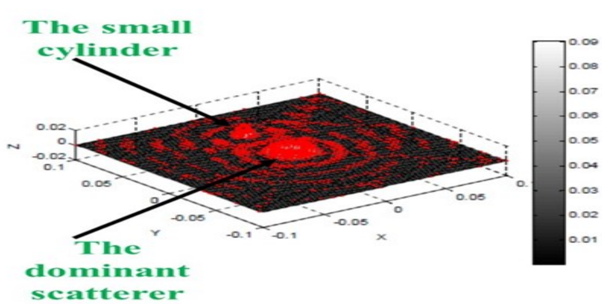

Fig. 9 The radio frequency tomographic image of the two objects represented as cells vector[4]

Simulation Evaluation:

By combining figures 4 and 7 together we can determine the control flow graph and the data flow graph paths, due to the space limitation, a figure illustrates the result of combining both figures is omitted. Interested readers are referred to [15,16,18,19] for more information about the data flow graph and the control flow graph. Once the software processes, which are displayed as the states shown in fig.4, and the interface messages between all states are known which are obtained from the approach developed in [4], our next step is to determine the performance parameters associated with the developed framework. These parameters are:

- **A. Tasks arrival rates λ.**
- **B. Number of tasks exists in each state before processing them N_i.**
- **C. Number of tasks move from the current state (S_i) to the new state (S_j) K_{ij}.**
- **D. Flow probabilities P_{ij}.**
- **E. Message multipliers β_{ij}, which are assumed to be unity.**
- **F. The computation and communication cost (service) times E(s).**

To utilize the performance parameters, at the early stage, we identify the input(s), output(s) and divide the framework into different components if possible as illustrated in fig. 10. There are one input, one output and 7 components (**one action, one sequence and five branches**).

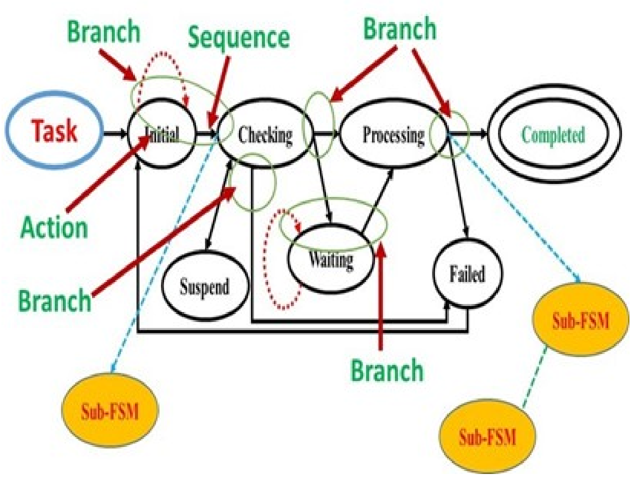

Fig. 10 system components

To find out the probabilities values for all states, Matlab simulation is used. We used it to determine how many tasks (N_i) exist first in each state and then how many tasks (k_{ij}) out of N_i are sent from state $\underline{S_i}$ to state $\underline{S_j}$. Note that, all these numbers should be known in advance either by obtaining them from actual tests (experiments/simulation) or given by the designers. The probability "P_i" is computed as follows:

$$P_i = K_{ij}/N_i \quad (10)$$

Multiple experiments were conducted to compute values for performance parameters to estimate the expected average response time, **a**verage **p**erformance **e**valuation, "**APE**".

A software structure, indicates the order in which the operations inside the framework are executed, is used in order to derive the average response time equations. The software structure is seen as the **C**omputation Structure **M**ethod (**CSM**) which consists of **D**ata **F**low **G**raph DFG and **C**ontrol **F**low **G**raph CFG as stated earlier.

To derive APE equations, we multiply each state time with its associated flow parameter; then sum all results after substituting all dependent flows with independent ones. The independent flows are defined as the flows that complete loop whereas the dependent flows are the remaining ones, which cannot complete loop. Now, estimating time needed to finish a task "process" in each state will be explained in detail.

The **A**ctual **A**verage **R**esponse **T**ime "***AART***" was found to be almost 78.017s after performing around 10000 iterations using Matlab 2016 on Windows 7 Enterprise as platform. To estimate EAP, we have the following quantities:

Tasks arrival rates λ = 2.46s/file, in total 9 files to be processed.

Number of tasks exist in the Initial State before processing them N1 = 2520.

Initial flow probabilities P_{ij} = [1 0 0 0 0 0], the Suspend State is included in the Checking State so that is why probability vector contains only 6 values instead of 7.

The computation and communication cost (service) times E(s) = 0.000370µs, which was obtained from a used workstation.

Table 1 depicts the specifications for the used workstation.

Table 1: Specifications of the platform

Platform Name	System Model and Type	CPU	Speed	RAM
Windows 7 Enterprise	ARM Build 64 bit	Intel Xeon E5-2697 V2	2.70Ghz	4 GB

The Initial State:

Fig. 11 illustrates CFG of the actual operations take place inside the Initial State as they are performed using Matlab to contrast energy function which is constructed by forming radio frequency image vector.

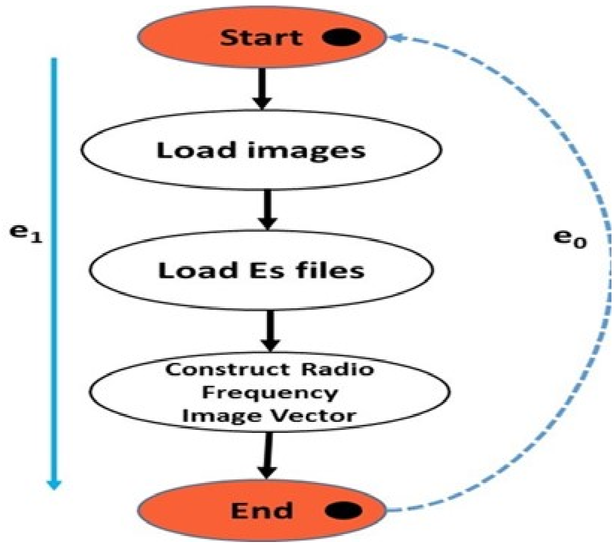

Fig. 11 CFG of the Initial State

The long bold arrow in fig. 11 represents the dependent flow while the dashed arrow indicates the independent one. Note that e0 = e1 = 1

$N_1 = 2520$

$K_{12} = 2520$

$P_{12} = K_{12} / N_1 = 1$

$C_{initial\ state} = 9.3745s.$

The Checking State:

$N_2 = 2520$

$K_{23} = 2520$

$K_{24} = 0$, *no task is sent to the Waiting state as stated earlier.*

$P_{23} = K_{12} / N_1 = 1$

$P_{24} = 0$, *all tasks are forwarded to the Processing state*

$C_{checking} = C_{applying\ MRL\ method\ to\ iteratively\ compute\ the\ contrast\ function\ energy} + C_{compare\ with\ the\ predefined\ threshold} = 2.48s$

$C_{applying\ MRL\ method\ to\ iteratively\ compute\ the\ contrast\ function\ energy} = 1.89$

$C_{compare\ with\ the\ predefined\ threshold} = 0.59$

Fig. 12 depicts the operations being performed in the Checking state.

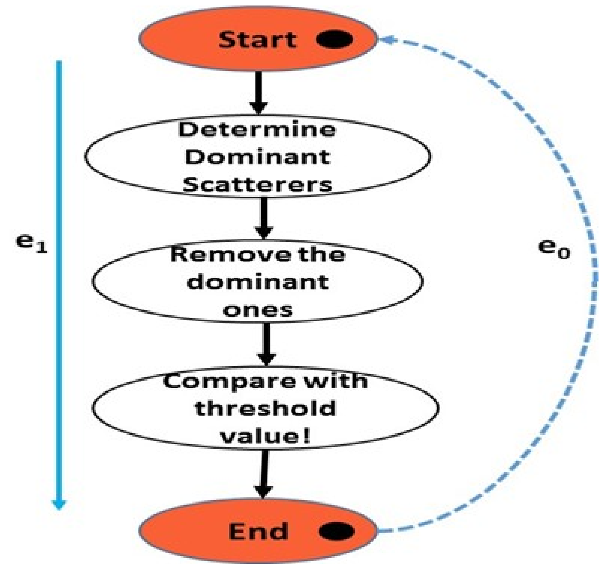

Fig. 12 CFG for the Checking state

Removing the dominant scatterers each time during the experiment magnifies the weak target features which is the main concern in this stage.
In the Processing state: from fig. 13, the equation for estimating the average response time is computed as follows:

$$C_{execution} = [(e_1 + e_4) * (C_{handling\ state} + C_{test})] + [e_4*C_{aborted}] + [(1+e_4)* C_{test}] \quad (11)$$

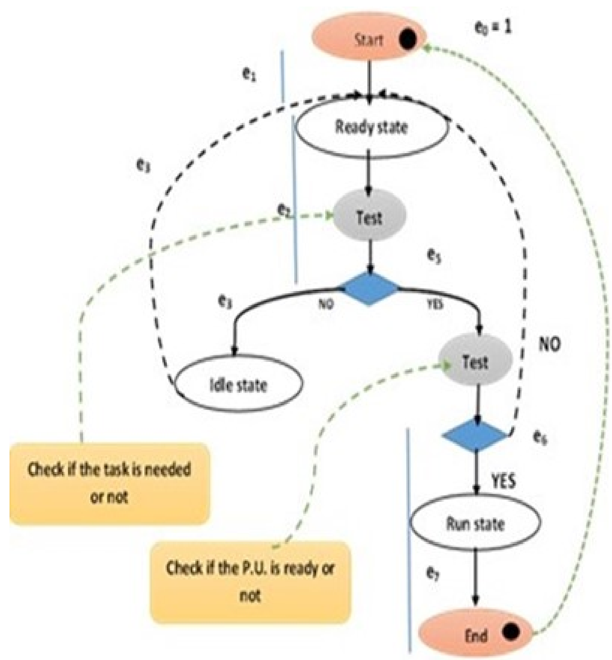

Fig. 13 CFG of the Handling state

Eq. (11) is obtained from CFG which is not shown due to the space limitation. Only CFG for the Handling state is illustrated in fig. 13. Substitute the value of eq. (12), showing below, into eq. (11) to estimate the value of the Processing state cost; the cost refers to the response time needed to complete the task in it.

$$C_{handling} = [(1 + e_3 + e_6) * (C_{ready} + C_{test})] + (e_3 * C_{idle}) + [(e_6 + 1) * C_{test}] + (1 * (C_{run})) \quad (12)$$

Note that the cost value obtained for each state represents the expected average time which is used for the computation in a Node View in the system level [1].

N3 = 2520

K36 = 2520

K35 = 0, no task was sent to the failed state since all tasks were handled by the PU.

P23 = K36 / N3 = 1

P35 = 0, all tasks were forwarded to the Completed state

From the simulation experiment, several quantities were obtained and used in the final estimation which were:

$C_{idle} = 0$, since the PU was fully occupied, $C_{ready} = 0.0003 \approx 0$ since its value is very small and can be neglected because there will be no effect on the final estimation.

C_{run} represents the computations and manipulation happen inside PU, thus,

$$C_{handling} = [(e_6 + 1) * C_{test}] + (1 * (C_{run})) \quad (13)$$

C_{test} is estimated using an "if statement" after running a program around 1000 times. Hence, $C_{test} = 0.00049$, the value is very small and can be included in the answer or neglected as done with C_{idle} and C_{ready}. We prefer to use it since it appears multiple times in the mathematical models "equations".

Substitute into eq. (13) to find that $\mathbf{C_{Processing\ state} = C_{Execution\text{-}state} = 72.5s}$.

Next step is to find the number of visit in each state using eq. (8), hence, the states: Checking, Processing and Completed were visited once as computed using Matlab platform. All flows "e_i" used in the model take either 0 or 0.5 since we use only single "if statement" as stated earlier. $C_{decision}$ is estimated the same way as C_{test}, so $C_{decision}$ is found to be approximately 0.00035.

So APE is estimated by substituting into eq. (9) to find that APE = $85.595 \approx 86s$.

The estimated error (***ER***) is computed as follows:

ER = $\left|\frac{AART-APE}{AART}\right| \approx 10\%$, in some applications, the ER is estimated as -9% < ER < +9% which seems acceptable.

The framework also tells us that the bottlenecks in the developed approach in [4] are as follows:

1. The algorithm took too much time in the Initial state by loading several files. This action will improve when a parallelization scheme is applied or an optimization technique is performed.
2. In the Processing state, Green functions delayed the output since many computations were performed there. The parallelization method or code optimization will help in reducing the computations time needed.

Lastly, initiating and drawing the outputs, figures, consumed too much processing power. Using either a powerful PU or a GPU with excellent capabilities will improve the performance for sure.

5. Conclusion and Future Work

This paper presented the developed framework to estimate the expected average response time "delay" in radar system which incorporated different levels of abstraction. The provided case study showed how the response time is estimated using the software structure within the framework. The framework is also capable of determining the places of bottlenecks inside the considered system.

The future work is to determine the average response time with a radar uses multiple PUs or any parallelization approach and finding the effect of rendering GPU(s) to take control on creating graphical task(s) such as drawing figures which are found to be the dominant factor. It takes about 62% of the average response time in the Processing state.

References

[1] Y. Guzel and A. Nassib, "Improved Signal Processing and Calibration Methods for GPR Tomography", IOSR Journal of Engineering (IOSRJEN), Vol. 6, Issue 7, pp. 48-56, July 2016.

[2] J. C. Roh and S. Aridhi, "Optimizing Modern Radar Systems Using Low-Latency, High-Performance FFT Coprocessors", Texas Instruments Incorporated, pp. 1-12, January 2016.

[3] Y. Li, X. Li, H. Wang, B. Deng and Y. Qin, "Performance Evaluation of Target Detection with a Near-Space Vehicle-Borne Radar in Blackout Condition", Proceedings of Sensors (Basel), Vol. 16, Issue 1, pp. 1-13, January 2016.

[4] M. Almutiry, M. C. Wicks, A. Nassib, Y. Guzel and L. L. Monte, "Extraction of Weak Target Features from Radar Tomographic Imagery", Proceedings of National Aerospace and Electronics Conference (NAECON), pp. 194-197, Dayton, Ohio, USA, June 2015.

[5] M. Almutiry, M. C. Wicks, T. Negishi, D. Erricolo and L. L. Monte, "Exploitation of Dominant Scatterers for Sidelobe Suppression in Radar Tomography", Proceedings of Signal Processing Symposium (SPSYmpo), pp. 1-4, June 2015.

[6] Y. Guzel, M. Almutiry, T. Tran, A. Nassib, M. C. Wicks, N. Al-faisali and L. L. Monte, "A Fast Matched-Filtered Approach for GPR", Proceedings of National Aerospace and Electronics Conference (NAECON), pp. 198-201, Dayton, Ohio, USA, June 2015.

[7] A. Nassib, M. Almutiry, Y. Guzel, M. C. Wicks and L. L. Monte, "FEKO Based ISAR Analysis for 3D Object Reconstruction", Proceedings of National Aerospace and

Electronics Conference (NAECON), pp. 188-193, Dayton, Ohio, USA, June 2015.
[8] A. K. Shrivas and A. Mudaliar, “Performance Evaluation of Radar Systems”, International Journal of Innovative Research in Computer and Communication Engineering (IJIRCCE), Vol. 3, Issue 7, pp. 6371-6377, July 2015.
[9] “Radar Performance Evaluation”, Intersoft of Electronics of Asia Pacific, October 2015.
[10] L. K. Cunha, J. A. Smith, M. Ln. Baech and W. F. Krajewski, “An Early Performance Evaluation of the Nexrad Dual-Polarization Radar Rainfull Estimates for Urban Flood Applications”, in Weather and Forecasting, Vol. 28, No. 6, pp. 1478-1497, December 2013.
[11] C. Du, “Performance Evaluation and Waveform Design for MIMO Radar, Ph.D. Dissertation Thesis, University of Edinburgh, March 2010.
[12] S. Zeng, “Performance Evaluation of Automotive Radars Using Carrier-Phase Differential GPS”, Proceedings of IEEE Transactions on Instrumentation and Measurements, Vol. 59, No. 10, pp. 2732-2741, October 2010.
[13] C. Sturm, S. Knorzer, T. Zwick and W. Wiesbeck, “Virtual Performance Evaluation of Automotive Radar Concepts in Realistic Traffic Environments”, Proceedings of International Conference on Electromagnetics in Advanced Applications, pp. 206-209, Torino, Italy, September 2009.
[14] G. Armbrecht, C. Zietz, E. Denicke and I. Rolfes, “A Flexible System Simulation for Antenna Performance Evaluation of Radar Level Measurements”, Proceedings of the 6th European Radar Conference (EURAD), pp. 513-516, Rome, Italy, October 2009.
[15] A. Alsheikhy, S. Han and R. Ammar, "Hierarchical Performance Modeling of Embedded Systems“, Computers and Communication (ISCC), 2015 20th IEEE Symposium on Computers and Communications, pp. 936-942, July 2015.
[16] A. Alsheikhy, S. Han and R. Ammar, "Delay and Power Consumption Estimation in Embedded Systems Using Hierarchical Performance Modeling”, 15th IEEE International Symposium on Signal Processing and Information Technology (ISSPIT), pp. 34-39, December 2015, Abu Dhabi, UAE.
[17] L. Chin, .S. Wei and G. Yu, ”Performance Evaluation of Embedded System Based on Behavior Expressions”, 2nd International Conference on Mechanical and Electronics Engineering (ICMEE), Vol. 1, pp. 253-256, 2010.
[18] D. Smarkusky, R. Ammar, I. Antonios and H. Sholl, “Hierarchical Performance Modeling for Distributed System Architectures,” Computer and Communications, 2000. Proceedings. ISCC 2000. Fifth IEEE Symposium, pp. 659–664, July 2000.
[19] R. Ammar, “Software Performance Analysis,” lecture notes, University of Connecticut, 1991.

Ahmed Alsheikhy, received the B.S. and M.S. degrees in Electrical and Computer Engineering from King Abdulaziz University 2004 and 2010, respectively. In 2016, he received the Ph.D. degree in Computer Science and Engineering from University of Connecticut, USA. During 2004-2010, he stayed in Technical Vocational Training Corporation (TVTC), Saudi Arabia to train military soldiers about computer networks and technical support. His research interests are on Performance Evaluation, Artificial Intelligence, Satellite and Radar communication systems and Internet of Things.

Muhannad Almutiry, received the B.S. degree in Electrical Engineering from Umm Alqura University 2007 and M.S. degree in 2010 from University of Dayton in Electrical Engineering. In 2016, he received Ph.D. in Electrical Engineering from University of Dayton. His research interests are on Satellite communications, Radar Frequency Tomography, Acoustic AUV Detection, Radar Sensing, Detection and Estimation and Artificial Intelligence.